MOLECULAR AND CELLULAR BIOLOGY, Aug. 2005, p. 6391–6403 Vol. 25, No. 15
0270-7306/05/$08.00+0 doi:10.1128/MCB.25.15.6391–6403.2005

Intracellular Reactive Oxygen Species Activate Src Tyrosine Kinase during Cell Adhesion and Anchorage-Dependent Cell Growth†

Elisa Giannoni,[1] Francesca Buricchi,[1] Giovanni Raugei,[1,2] Giampietro Ramponi,[1,2] and Paola Chiarugi[1,2]*

Department of Biochemical Sciences, University of Florence, V.le Morgagni 50, 50134 Florence, Italy,[1] and Center for Research, Transfer and High Education, Study at molecular and clinical level of chronic, inflammatory, degenerative and neoplastic disorders for the development of novel therapies, Florence, Italy[2]

Received 27 December 2004/Returned for modification 16 February 2005/Accepted 4 May 2005

Src tyrosine kinases are central components of adhesive responses and are required for cell spreading onto the extracellular matrix. Among other intracellular messengers elicited by integrin ligation are reactive oxygen species, which act as synergistic mediators of cytoskeleton rearrangement and cell spreading. We report that after integrin ligation, the tyrosine kinase Src is oxidized and activated. Src displays an early activation phase, concurrent with focal adhesion formation and driven mainly by Tyr527 dephosphorylation, and a late phase, concomitant with reactive oxygen species production, cell spreading, and integrin-elicited kinase oxidation. In addition, our results suggest that reactive oxygen species are key mediators of in vitro and in vivo v-Src tumorigenic properties, as both antioxidant treatments and the oxidant-insensitive C245A and C487A Src mutants greatly decrease invasivity, serum-independent and anchorage-independent growth, and tumor onset. Therefore we propose that, in addition to the known phosphorylation/dephosphorylation circuitry, redox regulation of Src activity is required during both cell attachment to the extracellular matrix and tumorigenesis.

The activation of integrins by the binding of ECM ligands (i.e., fibronectin, vitronectin, and laminin) induces many cellular responses, including attachment, spreading, migration, proliferation, and survival (27). Recently, we demonstrated that integrin engagement induces a transient increase in intracellular reactive oxygen species that peaks at 45 min of cell adhesion. This oxidative burst is at least threefold greater than that arising after growth factor stimulation (10). Intracellular ROS generated following integrin engagement are necessary for integrin signaling during fibroblast adhesion and spreading. 5′-LOX is mainly responsible for integrin-mediated ROS generation, with NADPH oxidase playing a marginal role. ROS are also central to the integration of signals from integrin and GFs, acting as synergistic mediators for each signaling pathway through both p125FAK (10) and Rho (24) redox regulation.

Important observations on the role of ROS as physiological regulators of tyrosine kinase receptor signaling cascades have shed new light on the possible mechanisms underlying the growth-regulating and tumor-promoting activities of ROS and on the antiproliferative and antitumoral action of some antioxidant agents (1). A growing body of evidence indicates that GF-induced oxygen species are necessary for optimal propagation of mitogenic and antiapoptotic signals through mechanisms that are incompletely understood.

The effect of ROS production is the reversible oxidation of proteins (13). Thiols, by virtue of their ability to be reversibly oxidized, are recognized as key targets of oxidative stress. Redox-sensitive proteins include protein tyrosine phosphatases, as their active-site cysteines are the targets of specific oxidation by various oxidants, including H_2O_2. This modification can be reversed by intracellular reducing agents (35). The inhibition exerted by ROS on PTPs helps to propagate receptor tyrosine kinase signals mediated by protein tyrosine phosphorylation, generally associated with a proliferative stimulus (7, 8).

Besides PTP inhibition, ROS up-regulate intracellular protein tyrosine phosphorylation by specific oxidation of cysteine SH groups on protein tyrosine kinases, thus inducing a conformational change necessary for their activation. H_2O_2 has been shown to mediate the activation of the epidermal GF receptor in lysophosphatidic acid-treated HeLa cells (12), the activation of Janus kinases in platelet-derived GF-treated Rat-1 cells (28), and the activation of protein kinase B in angiotensin II-treated vascular smooth muscle cells (32). The kinase-activating role of H_2O_2 in these cells was demonstrated by blocking H_2O_2 production with an NADPH oxidase inhibitor, namely, diphenylene iodonium, by preventing H_2O_2 accumulation with *N*-acetylcysteine or PEG catalase, or by introducing exogenous H_2O_2. ROS production induced by UV irradiation caused the dimerization and activation of the receptor tyrosine kinase Ret (22). This event is mediated by the formation of a disulfide bond between the Cys720 residues of each monomer, leading dimerized receptors to autophosphorylation resulting in their activation. This cysteine residue is highly conserved in various nonreceptor protein tyrosine kinases, including Abl, Src, and Lck, suggesting that it might also play a role in the activation of these enzymes.

Src family kinases are critically involved in the control of cytoskeletal organization and in the generation of integrin-dependent signaling responses in fibroblasts, inducing tyrosine phosphorylation of many signaling and cytoskeletal proteins

* Corresponding author. Mailing address: Dipartimento di Scienze Biochimiche, Viale Morgagni 50, 50134 Firenze, Italy. Phone: 39-055-4598343. Fax: 39-055-4498905. E-mail: paola.chiarugi@unifi.it.

† Supplemental material for this article may be found at http://mcb.asm.org/.

(31). The activity of the Src family of tyrosine kinases is tightly controlled by inhibitory phosphorylation of a carboxy-terminal tyrosine residue (Tyr527 in chicken c-Src). This phosphorylation induces an inactive conformation in the kinase through the subsequent intramolecular binding with its SH2 domain. The closed/inactive state is converted to the open/active state through Tyr527 dephosphorylation (11). While the dephosphorylation of the inhibitory tyrosine in lymphocytes appears to be performed by CD45 tyrosine phosphatase (19), during integrin-mediated responses the receptor protein tyrosine phosphatase α is responsible for Src family kinase activation by the dephosphorylation of Tyr527 (29). After the dephosphorylation of Tyr527, the conformational change promotes autophosphorylation at Tyr416 which, in turn, leads to enhanced Src kinase activity and to its complete activation (5, 36). SH3 domain interaction with the linker connecting the SH2 domain with the catalytic domain, leading to negative control of activity, has been proposed as a third mode of regulation of Src kinase (15).

We report here that c-Src is oxidized in response to cell attachment to the ECM and that this modification enhances kinase activity. We also show that the oxidation of v-Src is a key step in the acquisition of invasivity and anchorage/GF-independent growth in v-Src-transformed cells.

MATERIALS AND METHODS

Abbreviations. BIAM, *N*-(biotinoyl)-*N*′-(iodoacetyl)ethylenediamine; DTT, dithiothreitol; DCF-DA, 2′,7′-dichlorofluorescein diacetate; ECM, extracellular matrix; GF, growth factor; G/O, glucose oxidase; IAA, iodoacetic acid; 5′-LOX, 5′-lipoxygenase; PEG, polyethylene glycol; PTP, protein tyrosine phosphatase; NDGA, nordihydroguaiaretic acid; NAC, *N*-acetyl cysteine; ROS, reactive oxygen species; R-PTPα, receptor PTPα; MMP, matrix metalloprotein; PIPES, piperazine-*N*,*N*′-bis(2-ethanesulfonic acid); SDS, sodium dodecyl sulfate; PAGE, polyacrylamide gel electrophoresis; HRP, horseradish peroxidase; RIPA, radioimmunoprecipitation assay; cRIPA, complete RIPA; wt, wild type; FCS, fetal calf serum; FBS, fetal bovine serum; PBS, phosphate-buffered saline; SD, standard deviation.

Cell lines, reagents and constructs. Unless otherwise specified, all reagents were obtained from Sigma-Aldrich. NIH 3T3 cells were from the American Type Culture Collection. R-PTPα$^{-/-}$ and R-PTPα wild-type cells, a generous gift of Jan Sap (New York University School of Medicine), are embryonic fibroblasts derived from R-PTPα knockout mice and normal (control) mice, respectively. All antibodies were from Santa Cruz Biotechnology, except for the specific anti-phospho-Src (Tyr416) and anti-phospho-Src (Tyr527) antibodies, which were from Cell Signaling, and for the anti-phosphotyrosine 4G10 and anti-c-Src immunoglobulin G used for c-Src kinase assay, which were from Upstate Biotechnology. BIAM and 5′-iodoacetamide fluorescein were obtained from Molecular Probes. HRP-streptavidin was from Bio-Rad. The eukaryotic expression vector encoding the chicken c-Src was a generous gift of Andrea Graziani (University of Novara).

Site-directed mutagenesis and transfections. Site-directed mutagenesis was performed using the QuikChange site-directed mutagenesis kit (Stratagene) and confirmed by sequencing. Codons for five cysteine residues in the coding sequence of pSG5c-Src (C238, C245, C400, C487, and C498) were replaced by alanine codons. In addition, C245 and C487 were mutated to alanines in the coding sequence of pSG5c-SrcY527F. wt c-Src, its oncogenic mutant c-SrcY527F, and their Cys-to-Ala mutants, inserted into the pSG5 vector, were transiently or stably transfected into NIH 3T3 cells using PolyFect transfection reagent (QIAGEN) according to the manufacturer's protocol. The efficiencies of transient transfections were equalized, and overexpression was maintained in the range of 8- to 10-fold by transfecting 4 μg of DNA/10-cm dish.

Cell cultures. NIH 3T3 cells and NIH 3T3 cells stably overexpressing the oncogenic form v-Src (3T3 v-Src) were routinely cultured in Dulbecco's modified Eagle's medium supplemented with 10% FCS at 37°C in a 5% CO_2 humidified atmosphere. R-PTPα wt and R-PTPα$^{-/-}$ cells were cultured in Dulbecco's modified Eagle's medium supplemented with 10% FBS at 37°C and 10% CO_2.

Cell adhesion. NIH 3T3 or 3T3 v-Src cells (1×10^6) were serum starved for 24 h before detaching with 0.25% trypsin for 1 min. Trypsin was blocked with 0.2 mg/ml soybean trypsin inhibitor, and cells were resuspended in 2 ml/10-cm dish of serum-depleted medium, maintained in suspension for 30 min at 37°C, and then directly seeded for the times indicated below onto 10-cm dishes precoated overnight with 10 μg/ml human fibronectin and washed twice with PBS. Control cells were kept in suspension by plating them onto dishes pretreated with 1 mg/ml of bovine serum albumin in culture medium, thus preventing cell adhesion to the dish.

Assay of intracellular H_2O_2. Intracellular production of H_2O_2 was assayed as previously described (10). Five minutes before the end of the incubation time, adherent or suspended cells were treated with 5 μg/ml DCF-DA. After PBS washing, cells were lysed in 1 ml of RIPA buffer and analyzed immediately by fluorescence spectrophotometric analysis at 510 nm. Data were normalized to total protein content.

Immunoprecipitation and immunoblot analysis. NIH 3T3 cells (1×10^6) were seeded in 10-cm plates in Dulbecco's modified Eagle's medium supplemented with 10% FCS. Cells were serum starved for 24 h and then stimulated with or without 100 mU/ml G/O for 15 min. Alternatively, serum-starved cells were detached, resuspended, and replated onto fibronectin-coated dishes as described above. Cells were then lysed for 20 min on ice in 0.5 ml of cRIPA lysis buffer (50 mM Tris-HCl, pH 7.5, 150 mM NaCl, 1% Triton X-100, 2 mM EGTA, 1 mM sodium orthovanadate, 1 mM phenylmethylsulfonyl fluoride, 0.1% SDS, 0.5% sodium deoxycholate, 10 μg/ml aprotinin, and 10 μg/ml leupeptin). All samples were divided into two halves used for direct immunoblot analysis and for normalization. For each immunoblot experiment, 25 μg of total protein was used. Each sample (1 mg/ml) was immunoprecipitated with 2 μg of specific antibodies. Immunocomplexes were then separated by SDS-PAGE and transferred onto nitrocellulose. Immunoblots were incubated in 1% bovine serum albumin, 10 mM Tris-HCl, pH 7.5, 1 mM EDTA, and 0.1% Tween 20 for 1 h at room temperature; probed with specific antibodies; and developed with an enhanced chemiluminescence kit. Densitometric analysis of the results was performed with Chemidoc quantitation analysis software (Bio-Rad).

Detection of Src oxidation by carboxymethylation. NIH 3T3 or 3T3 v-Src cells were cultured at 60% confluence in 10-cm dishes (1×10^6 per dish) and then exposed to the above-mentioned stimuli (G/O and cell adhesion). The medium was then removed, and the cells were frozen rapidly in liquid nitrogen. The frozen cells were then exposed to 0.5 ml of lysis buffer (50 mM Tris-HCl, pH 7.5, 150 mM NaCl, 0.5% [vol/vol] Triton X-100, 10 μg/ml aprotinin, and 10 μg/ml leupeptin; the buffer was rendered free of oxygen by bubbling with nitrogen gas at a low flow rate for 20 min) containing 100 μM BIAM. After sonication in a bath sonicator for three periods of 1 min each separated by 30-s intervals, the cell lysates were incubated for 15 min at room temperature. Lysates were then clarified by centrifugation and subjected to immunoprecipitation with c-Src specific antibodies.

For double carboxymethylation with IAA and BIAM labeling, NIH 3T3 cells were treated as described above, with the exceptions that the lysis buffer contained 30 mM IAA instead of BIAM and that the incubation was for 15 min at 37°C. Cells were treated as described above, and Src kinase immunoprecipitated with c-Src specific antibodies. After the washings, immunoprecipitated Src protein was denatured with the addition of 200 μl of lysis buffer containing 8 M urea and 30 mM IAA and incubated for 15 min at 37°C to assure the carboxymethylation of nonexposed reduced cysteines. Proteins were precipitated with cold acetone/HCl/H_2O (at a ratio of 92:2:10) to remove IAA. After centrifugation, the pellets were resuspended in 50 μl lysis buffer containing 8 M urea. Thereafter, 3.5 mM dithiothreitol was added to half of each sample, and the second carboxymethylation with biotinylated probe (10 mM BIAM in lysis buffer for 15 min at 37°C) was performed to detect previously oxidized cysteines. Immunocomplexes labeled with BIAM were detected with HRP-conjugated streptavidin and ECL.

In vitro Src kinase assay. An in vitro c-Src kinase assay was performed using enolase as a substrate as described elsewhere (2). Briefly, 1×10^6 suspended or adherent NIH 3T3 cells were lysed in 0.5 ml cRIPA lysis buffer, and c-Src was immunoprecipitated from 1 mg of total protein with anti-c-Src immunoglobulin G (Upstate Biotechnology). Each immunoprecipitate was assayed for c-Src kinase activity by incubating with 10 μl of reaction buffer (20 mM PIPES, pH 7.0, 10 mM $MnCl_2$, 10 μM Na_3VO_4), 1 μl of freshly prepared acid-denatured enolase (Sigma) (5 μg of enolase and 1 μl of 50 mM HCl incubated at 30°C for 10 min and then neutralized with 1 μl of 1 M PIPES, pH 7.0), and 10 μCi of [γ-^{32}P]ATP. After 10 min of incubation at 30°C, reactions were terminated by the addition of 2× SDS sample buffer, and samples were subjected to 10% SDS-PAGE. Coomassie staining was performed to confirm the presence of equal amounts of enolase. The gel was dried and analyzed with a Cyclone system (Perkin-Elmer).

Alternatively, c-Src kinase activity was evaluated by analysis of the Tyr416 autophosphorylation level with specific anti-phospho-Src (Tyr416) antibodies.

Zymography. Metalloprotease zymography was assessed as described elsewhere, with minor modifications (23). Briefly, 3×10^5 cells of the indicated type were allowed to grow for 72 h in culture medium alone or supplemented every 24 h with 10 μM NDGA. Twenty microliters of culture medium was collected every 24 h and added to sample buffer (0.4% SDS, 2% glycerol, 10 mM Tris-HCl, pH 6.8, 0.001% bromphenol blue). The samples were separated on an 8% SDS gel containing 0.1% gelatin. After electrophoresis, the gel was washed twice with 2.5% Triton X-100 and once with reaction buffer (50 mM Tris-HCl, pH 7.5, 200 mM NaCl, 5 mM $CaCl_2$). The gel was incubated overnight at 37°C with freshly added reaction buffer and stained with Coomassie blue solution.

In vitro invasion assay. The in vitro invasion assays were carried out as described previously (37). 3T3 v-Src cell invasion was assayed with the Transwell system of Costar, equipped with 8-μm-pore-size polyvinylpyrrolidone-free polycarbonate filters (diameter, 13 mm). Matrigel (BD Biosciences) was diluted (30 μg in 100 μl of H_2O), added to the top chamber, allowed to solidify for 1 h at 37°C, and air dried for 16 h. The Matrigel barrier was reconstituted with 100 μl of Dulbecco's modified Eagle's medium for 2 h at 37°C prior to use. Cells were loaded into the upper compartment (5×10^4 cells in 300 μl) in serum-deprived growth medium. The Matrigel invasion chambers were placed into six-well culture dishes containing 1 ml of Dulbecco's modified Eagle's medium with 20% serum as a chemoattractant. After 24 h of incubation at 37°C, noninvading cells and the Matrigel layer were mechanically removed using cotton swabs, and the microporous membrane containing the invaded cells was fixed in 96% methanol and stained with Diff-Quick staining solutions. Chemotaxis was evaluated by counting the cells that migrated to the lower surfaces of the polycarbonate filters. The numbers of cells in six randomly chosen fields were determined for each filter, and the counts were averaged (means ± SD).

Serum-independent cell growth assay. NIH 3T3 or 3T3 v-Src cells (2×10^4) were seeded in gelatin-coated 24-multiwell plates in 0.5% serum with or without 10 μM NDGA or 20 mM NAC. Fresh NDGA and NAC were added daily. Cell growth was stopped by removing the medium and adding a 0.5% crystal violet solution in 20% methanol. After 5 min of staining, the fixed cells were washed with PBS and solubilized with 200 μl/well of 0.1 M sodium citrate, pH 4.2. The absorbance at 595 nm was evaluated using a microplate reader.

Soft agar assay. For measurement of anchorage-independent growth, 4×10^4 3T3 v-Src cells were suspended in 0.3% Bacto agar (Difco) growth medium containing 10% FBS in the presence or absence of antioxidants (20 mM NAC and 10 μM NDGA), seeded onto a solidified base of growth medium containing 0.6% agar, and overlaid with 1 ml of growth medium. After 24 h, media containing 10% FBS were added to each 35-mm dish and renewed twice weekly. The antioxidants were added to the solid underlay, the overlay agar media, and the liquid top layer. Colonies were scored after 2 weeks, and all values were determined in triplicate. Photographs were taken with a phase-contrast microscope (Nikon).

Tumorigenicity assay. Tumorigenicity was assayed by the injection of 10^5 cells into nude mice (NIH 3T3 *nu*/*nu*, female, and 6 weeks of age) subcutaneously over the lateral thorax. Animals were examined twice weekly and sacrificed 20 days later. Lung metastases and the neoplastic nature of local tumors were confirmed by histologic examination.

RESULTS

c-Src is oxidized in vivo. A powerful tool for the identification of redox-regulated proteins during integrin-mediated cell adhesion is the labeling of cells with BIAM. BIAM is a sulfhydryl-modifying reagent that selectively probes the thiolate form of cysteine residues in the reduced state. NIH 3T3 cells were exposed to an exogenous oxidative stress generated by G/O treatment, and then the lysates were labeled with BIAM. c-Src was immunoprecipitated, and the biotinylated/reduced fraction of the kinase was revealed with an HRP-streptavidin immunoblot. The results indicate that c-Src is directly oxidized during G/O treatment (Fig. 1A). To analyze the redox state of the kinase in response to integrin-mediated cell adhesion, cells were exposed to fibronectin. We previously reported that ROS are maximal at 45 min after integrin engagement (10). Our results indicate that during integrin-mediated cell adhesion, c-Src is markedly oxidized (Fig. 1B). We verify the redox sensitivity of c-Src by use of an additional SH-modifying agent, namely, 5′-iodoacetamide fluorescein, and with antifluorescein immunoblotting (9), obtaining similar results (data not shown). To confirm this observation and exclude the possibility that BIAM labeling was affected by cysteine accessibility, we analyzed BIAM labeling on urea-denatured proteins. We utilized an additional method which probes oxidized cysteines instead of the reduced moieties, based on a two-step carboxymethylation. We first treated cell lysates with IAA to block reduced cysteines, and then c-Src was immunoprecipitated from all samples and denatured by 8 M urea. Each sample was then treated or not with DTT in order to reduce the cysteines that were oxidized in vivo and not carboxymethylated with the first treatment with IAA. Finally, the samples were treated with BIAM to label the newly reduced cysteines. The omission of DTT treatment before BIAM labeling completely abolishes the streptavidin signal (data not shown). The results show a large increase in BIAM labeling due to cell adhesion, confirming that c-Src is oxidized during integrin engagement (Fig. 1C).

We recently reported that 5′-LOX is the predominant system involved in oxidant generation during integrin-mediated cell adhesion (10). The use of the LOX-specific inhibitor NDGA prevents the oxidation of c-Src in response to integrin engagement, suggesting the role of cell adhesion-generated ROS in the oxidation of the kinase (Fig. 1D). In order to confirm a direct role of ROS produced in response to cell adhesion, we report that PEG catalase treatment during integrin-mediated cell adhesion prevents Src oxidation (Fig. 1E).

Integrin-mediated c-Src oxidation is associated with an increase in kinase activity. The regulation of c-Src kinase activity has been much discussed. The current literature depicts the PTP-mediated dephosphorylation of Tyr527 as the activation step necessary to switch kinase activity on and the autophosphorylation of Tyr416 as an essential event for the completion of activation (11). To assess the role of Src oxidation in its enzymatic activity, we analyzed the cell adhesion-dependent autophosphorylation of Src Tyr416 during NDGA treatment. As indicated in Fig. 2A, the inhibition of the integrin-mediated ROS burst reduced the autophosphorylation of Tyr416 to its basal level. An in vitro kinase assay on immunoprecipitated c-Src confirms that NDGA treatment eliminates the enhancement of kinase activity during cell adhesion (Fig. 2B). Together, these findings implicate the oxidants produced by integrin engagement as coregulators of Src tyrosine kinase activation. To investigate a regulatory function for Src oxidation during cell adhesion, we analyzed (i) the association between Src and the focal adhesion tyrosine kinase (p125FAK) and (ii) p125FAK tyrosine phosphorylation during NDGA treatment (Fig. 2C). Once again, blockage of the ROS-generating system during cell adhesion abolishes p125FAK recruitment and activation, reinforcing our hypothesis of a key role for Src oxidation in the transduction of the adhesive signal.

Identification of the redox-regulated cysteines in c-Src. To identify the cysteine(s) responsible for Src oxidation, we chose Cys238, -245, -400, -487, and -498 as mutation targets on the basis of their strict conservation among all Src family members. Site-specific mutagenesis was performed, and wild-type and mutant c-Src kinases were expressed in NIH 3T3 cells. Suspended and adherent cells were labeled with BIAM and re-

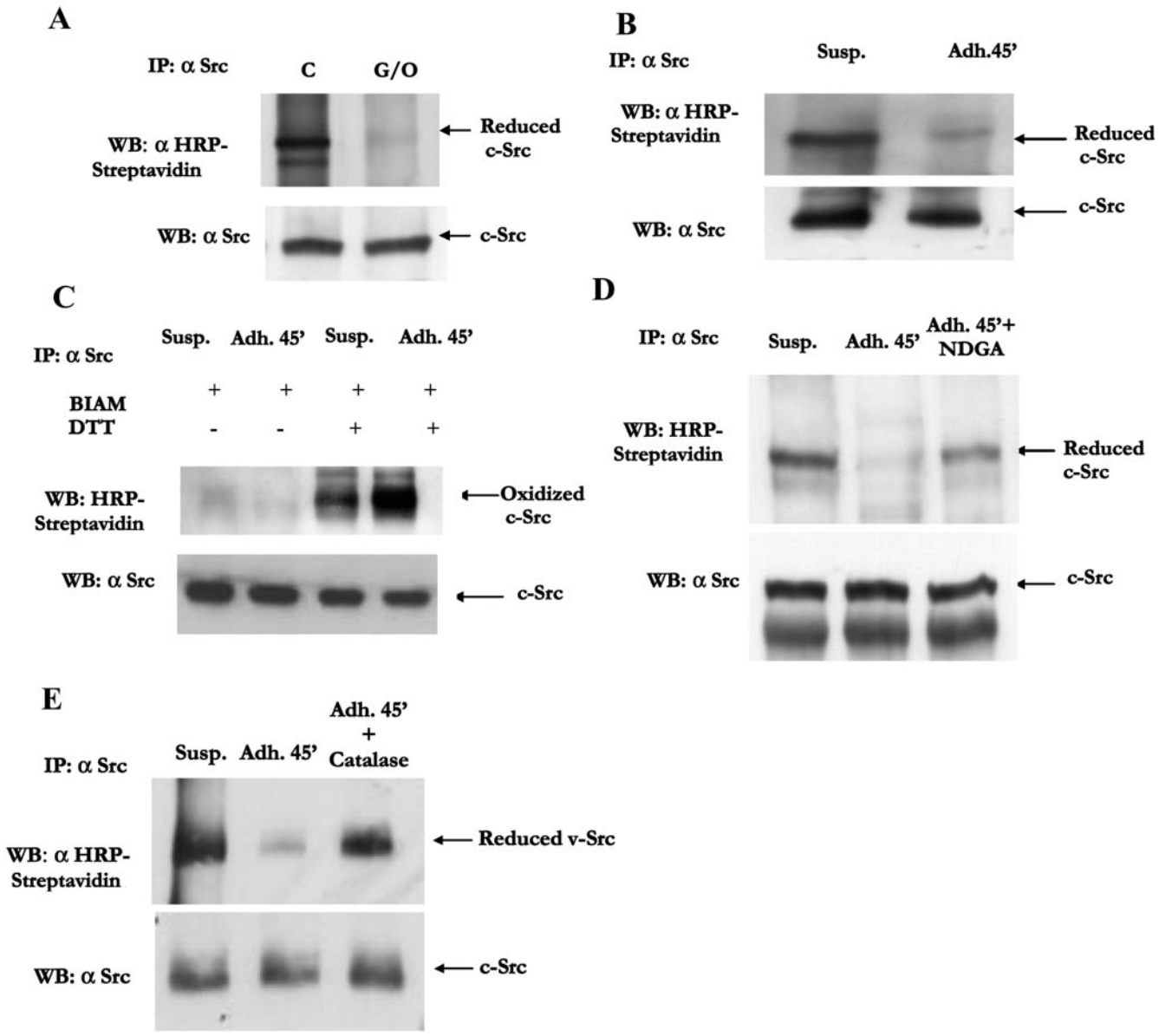

FIG. 1. c-Src is oxidized during G/O treatment and integrin-mediated cell adhesion. (A) NIH 3T3 cells were serum starved for 24 h and then treated with or without G/O for 15 min. Cell lysates were labeled with BIAM, and c-Src was immunoprecipitated (IP) from each sample. HRP-streptavidin immunoblotting was performed to evaluate the reduced form of c-Src. With a half of each sample, Western blotting (WB) with anti-c-Src antibodies was performed for normalization. (B) NIH 3T3 cells were serum starved for 24 h and then detached and maintained in suspension with gentle agitation for 30 min at 37°C. Cells were then kept in suspension or replated onto fibronectin-precoated dishes for 45 min. c-Src was immunoprecipitated from BIAM-labeled cell lysates. HRP-streptavidin and c-Src immunoblotting was performed. (C) NIH 3T3 cells were serum starved for 24 h, detached, and maintained in suspension for 30 min at 37°C. Cells were then kept in suspension or replated onto fibronectin-precoated dishes for 45 min. Prior carboxymethylation with IAA was carried out, and urea-denatured c-Src was immunoprecipitated from subsequent BIAM-labeled cell lysates. Samples were treated with DTT before BIAM labeling. HRP-streptavidin and anti-c-Src immunoblotting was performed. (D) NIH 3T3 cells were treated as described for panel B (right lanes), except that they were pretreated for 30 min before adhesion with or without 10 μM NDGA to inhibit the 5′-LOX-mediated synthesis of ROS. (E) NIH 3T3 cells were treated as described for panel B (right lanes), except that they were treated during adhesion with 1 μg/ml of PEG catalase. Cell lysates were labeled with 40 μM BIAM, and c-Src was immunoprecipitated from each sample. The samples were split in two, and HRP-streptavidin and anti-Src immunoblotting was performed. All data are representative of at least three independent experiments.

duced. c-Src was quantified by HRP-streptavidin immunoblotting. As shown in Fig. 3A, wt and Cys238, Cys400, and Cys498 mutants are oxidized after 45 min of cell adhesion. In contrast, two mutants, i.e., Cys245 and Cys487, are insensitive to the oxidative burst produced in response to adhesion onto fibronectin. Analysis of oxidized c-Src during ECM contact by double carboxymethylation with IAA and BIAM confirms that the Cys245 and Cys487 mutants are not oxidized in response to adhesion (Fig. 3B). Consistent with their role in Src oxidation during adhesion, the Cys245 and Cys487 mutants are not ac-

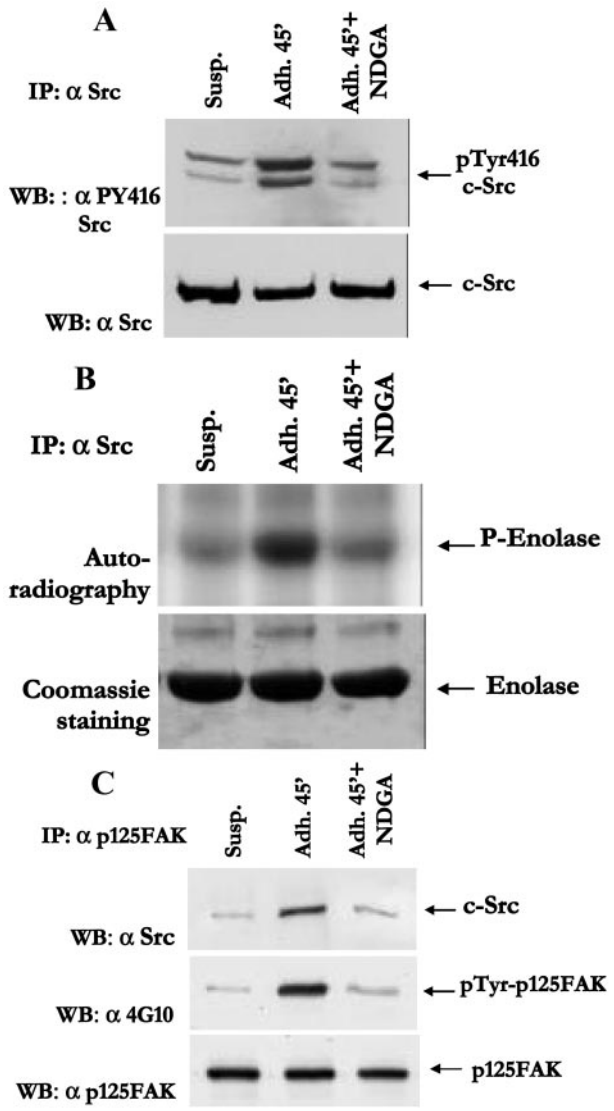

FIG. 2. c-Src activity and downstream signaling greatly increase upon adhesion-dependent ROS production. (A) NIH 3T3 cells (1×10^6) were serum starved for 24 h before detaching and maintained in suspension for 30 min at 37°C with or without 10 μM NDGA. Cells were then either kept in suspension or seeded onto fibronectin-treated dishes for 45 min. Integrin stimulation was stopped by collecting cells in 0.5 ml of cold cRIPA lysis buffer. Twenty-five micrograms of total protein for each sample was separated by 10% SDS-PAGE, and immunoblotting (WB) was performed with anti-phospho-Src (Tyr416) and anti-Src antibodies (for normalization). (B) NIH 3T3 cells (1×10^6) were treated as described for panel A, except that c-Src was immunoprecipitated (IP) from 1 mg of total protein. Each immunoprecipitate was assayed for c-Src kinase activity on enolase. The samples were subjected to 10% SDS-PAGE, and the gel was then dried and analyzed with a Cyclone system (Perkin-Elmer). A Coomassie staining analysis was also performed to confirm equal amounts of enolase present, and an anti-Src immunoblotting was performed for normalization. (C) To evaluate the amount of Src/p125FAK association and the level of p125FAK phosphorylation, cells were treated as described for panel A, except that p125FAK was immunoprecipitated from 1 mg of total protein. Immunoprecipitates were split in two and loaded in 10% SDS-PAGE gels, and anti-Src and anti-phosphotyrosine 4G10 immunoblotting was performed. The anti-4G10 blot was then stripped and reprobed with anti-p125FAK antibodies for normalization. All the reported experiments are representative of three others with similar results.

tivated upon cell adhesion on ECM, as indicated by anti-P416 immunoblotting (Fig. 3C). We also report that the Cys245 and Cys487 mutants are not activated upon in vitro hydrogen peroxide treatment (see Fig. S1 in the supplemental material). We further analyzed the sensitivity to Tyr527 dephosphorylation of Src mutants. The results demonstrate that all Src mutants remain perfectly independent from integrin-elicited Tyr527 dephosphorylation, suggesting that these cysteines do not play any role in this step (Fig. 3D). Finally, we show that Src oxidation of these particular cysteines has a key role in downstream signaling control, as the Cys245 and Cys487 mutants fail to activate p125FAK (Fig. 3E). Taken together, these results identify Cys245 and Cys487 as the main targets of c-Src oxidation during cell adhesion and the engagement of integrins by the ECM.

Early and late Src activation during ECM cell adhesion. To investigate the function of ROS generated during integrin engagement in Src activation, we compared the phosphorylation of both c-Src regulatory tyrosines, namely, Tyr527 and Tyr416, during early and late integrin-mediated cell adhesion. Phosphorylation of Tyr416 displays an early increase at 10 min and a second and more pronounced boost at 45 min, followed thereafter by a definitive decrease (Fig. 4). Conversely, the phosphorylation of inhibitory Tyr527 displays a decrease concurrent with early ECM contact (10 min) and recovers only after the cells have completely spread (90 to 120 min). We previously reported that in NIH 3T3 cells the generation of ROS due to integrin engagement peaks at 45 min after ECM contact, when cells are spreading and organizing their cytoskeletons (10). Overall, there is temporal concordance of additional Tyr416 phosphorylation, continued Tyr527 dephosphorylation, and initiation of cell spreading with ROS production and Src oxidation at 45 min.

The dephosphorylation of the inhibitory P-Tyr527 in response to ECM contact is in agreement with previously reported data describing a role of R-PTPα in the early activation of Src (29, 33). We herein provide further evidence of the role of R-PTPα in the early activation of Src tyrosine kinase upon integrin-mediated cell adhesion. We confirmed a role of R-PTPα in the early dephosphorylation (i.e., 10 min) of the Src-inhibitory Tyr527 by comparing fibroblasts derived from R-PTPα-deficient mice (R-PTPα$^{-/-}$) with those from R-PTPα-expressing mice (R-PTPα wt) (Fig. 5A). In addition, R-PTPα$^{-/-}$ cells exhibited a dramatic reduction of c-Src Tyr416 autophosphorylation in the early phase of cell adhesion compared to R-PTPα wt cells (Fig. 5B), in agreement with the proposed role of R-PTPα in the Tyr527 dephosphorylation-mediated transition of the kinase to an open/active conformation (29, 39). In contrast, the late activation of c-Src occurs in both cell lines, although the extent of kinase activation after 45 min of ECM contact is decreased in R-PTPα$^{-/-}$ fibroblasts. These findings indicate the involvement of R-PTPα mainly in the early phase of Src activation, in agreement with the kinetics of phosphorylation of its target P-Tyr.

To analyze the role of ROS-mediated oxidation in both the early and late activations of c-Src due to integrin-mediated cell adhesion, we analyzed the redox state of c-Src in cells upon ECM contact. Figure 5C shows that c-Src oxidation is very low during early adhesion (10 min) and reaches a maximum during late cell adhesion (45 min) and that it returns to baseline when

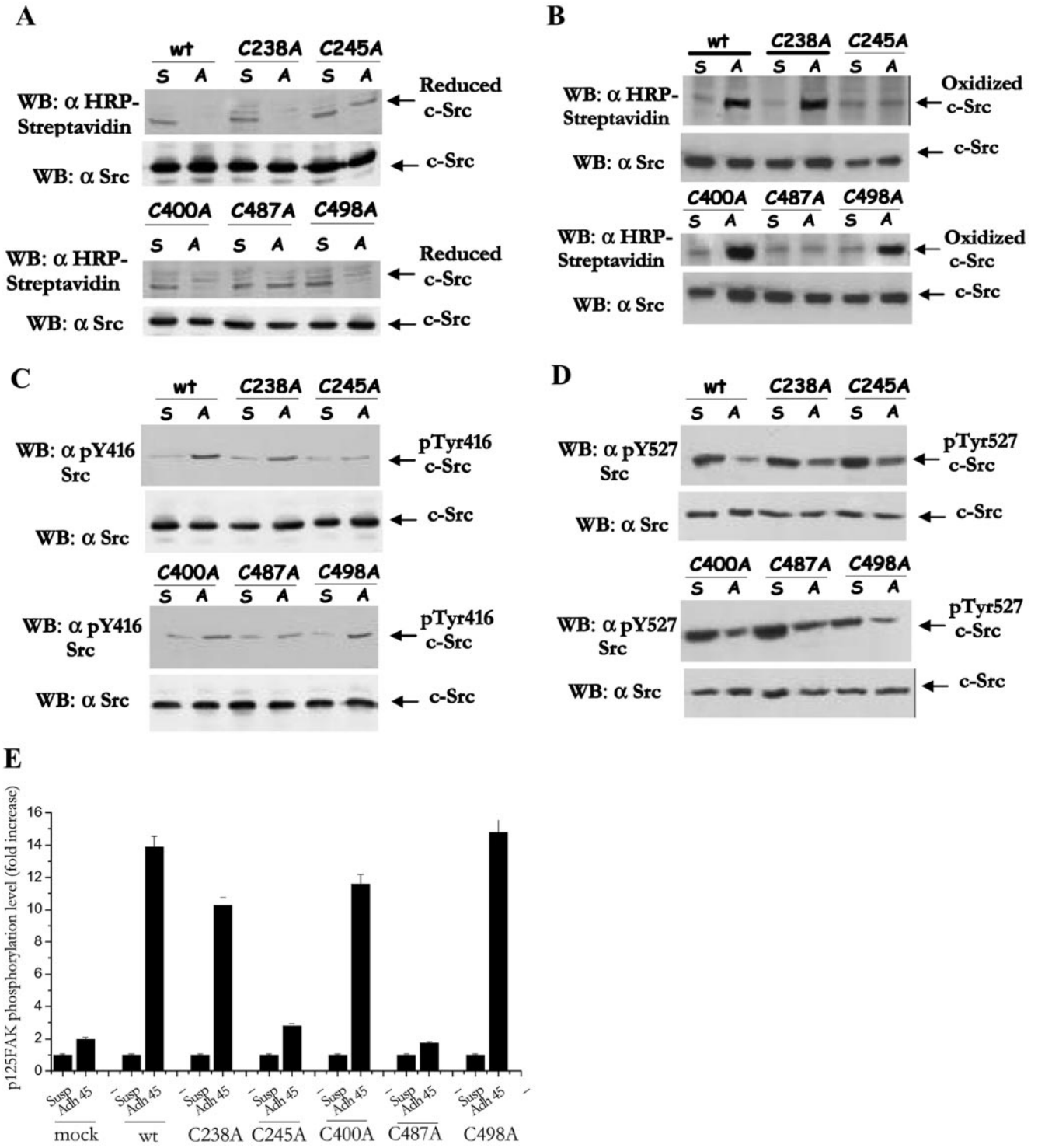

FIG. 3. Role of conserved cysteines in c-Src redox regulation. (A) NIH 3T3 cells were transiently transfected either with pSG5 encoding wt c-Src, with the five conserved cysteine-to-alanine mutants of the kinase (C238A, C245A, C400A, C487A, and C498A), or with the vector alone as a control. Twenty-four hours after transfection, cells were serum starved for an additional 24 h before being detached and maintained in suspension for 30 min at 37°C with gentle agitation. Cells were either kept in suspension or seeded onto fibronectin-treated dishes for 45 min. Cell lysates were labeled with BIAM, and c-Src was immunoprecipitated from each sample. Anti-HRP-streptavidin immunoblotting (WB) was performed to evaluate the wt and mutant c-Src redox states. (B) Cells were treated as described for panel A, except that double carboxymethylation with IAA and BIAM was performed to detect oxidized Src. Prior carboxymethylation with IAA was carried out, and urea-denatured c-Src was immunoprecipitated from subsequent BIAM-labeled cell lysates. HRP-streptavidin immunoblotting was performed. The blot was then stripped and reprobed with anti-c-Src antibodies for normalization. (C) To analyze Src activation, cells were treated as described for panel A, except that they were lysed in 0.5 ml of cold cRIPA lysis buffer. Twenty-five micrograms of total protein for each sample was separated by 10% SDS-PAGE, and immunoblotting was performed with anti-phospho-Src (Tyr416) antibodies. (D) To analyze Tyr527 dephosphorylation, cells were treated as

cells have already spread (120 min). Furthermore, when integrin-stimulated cells were treated with the antioxidant NDGA, which specifically inhibits the integrin-elicited ROS burst (10), there is no change in early Src activation, but the late phase of Src activation is completely eliminated (Fig. 5D). Therefore, ROS act only in the late phase of integrin-mediated cell adhesion, namely, when cells are spreading on the ECM. In addition, we analyzed the kinetics of c-Src activation in Cys245 and Cys487 mutants in response to ECM contact with respect to the wild-type enzyme. Early activation of c-Src, i.e., at 10 min from ECM contact, was maintained in both Cys245 and Cys487 mutants, while the late activation of the tyrosine kinase (45 min of cell adhesion) was dramatically impaired in both Cys245 and Cys487 mutant c-Src kinases (Fig. 5E). Taken together, these findings demonstrate a role of Src oxidation in the late activation of the kinase strictly concomitant with the peak of ROS production due to ECM contact.

The role of ROS in v-Src oncogenic properties. The production of large amounts of oxidants in tumor cells, including human tumors, in which the activation of Src has been causally linked to their tumorigenic potential, has been previously reported (3, 16, 30). We therefore analyzed the role of kinase activation via oxidation in the tumorigenic properties of the v-Src oncoprotein. In v-Src-transfected NIH 3T3 cells, the basal (not induced by cell adhesion) ROS level is increased by up to twofold, although it is only partially dependent upon ECM contact (Fig. 6A).To evaluate the role of ROS in v-Src-induced cell transformation, we analyzed the effect of both oxidative stress and antioxidant treatment on v-Src NIH 3T3 cells. v-Src is oxidized during the generation of an exogenous oxidative burst by G/O treatment, and the reversal of the redox potential by PEG catalase treatment leads to protein rereduction (Fig. 6B). v-Src oxidation, in agreement with the behavior of its cellular counterpart, c-Src, is likely associated with kinase activation, as indicated by the increase of Tyr416 autophosphorylation (Fig. 6C).

v-Src expression has been causally linked to the specific gain in tumorigenic properties in nontransformed fibroblasts. The expression of this oncoprotein leads to an invasive phenotype through increased expression of MMPs (17) and to the ability to grow in the absence of growth factor-supported media, ECM support, or both (14, 26). To address the possibility that ROS affect the invasivity of v-Src cells, we analyzed the susceptibility of both MMP expression and the ability of cells to move through a reconstituted Matrigel lamina to NDGA (Fig. 7A and B). In addition, the involvement of ROS in the regulation of Src-induced migration is confirmed by its sensitivity to PEG catalase (see Fig. S2 in the supplemental material). Our results suggested that ROS greatly affect the expression of MMPs and three-dimensional cell motility, thus defining a role for ROS in v-Src-induced invasivity potential. Serum- and anchorage-independent growth of v-Src3T3 was analyzed in the presence or absence of antioxidant treatments to determine

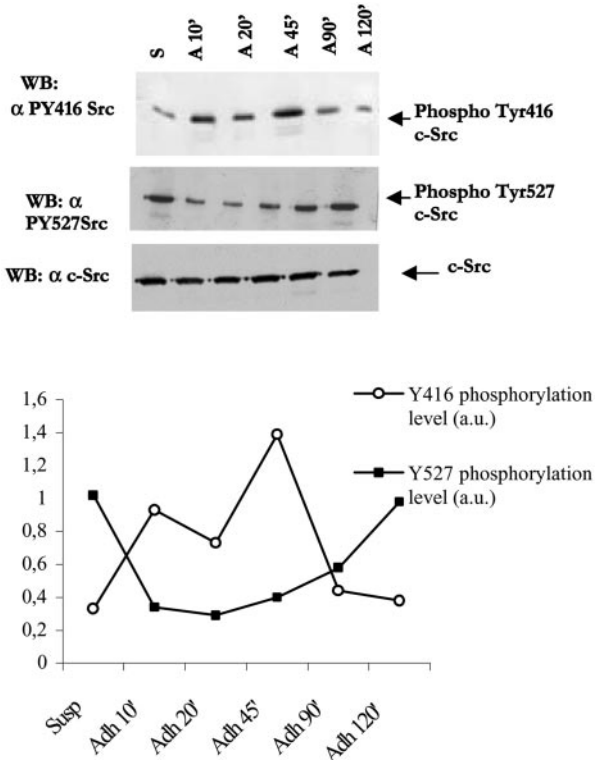

FIG. 4. Tyrosine phosphorylation of Tyr527 and Tyr416 during ECM contact. NIH 3T3 cells (1×10^6) were serum starved for 24 h before being detached and maintained in suspension for 30 min at 37°C with gentle agitation. Cells were either kept in suspension or seeded onto fibronectin-treated dishes for the indicated times. Twenty-five micrograms of total lysate in cRIPA buffer was separated by 10% SDS-PAGE, and immunoblotting (WB) was performed with anti-phospho-Src (Tyr416 or Tyr527) or with c-Src antibodies for normalization. Normalized values for the phosphorylation of each tyrosine are reported in the plot. S, suspended cells; A, adherent cells. The times (in min) of adherence are indicated.

the significance of ROS in relation to cell transformation. We used both NAC, a common cell-permeable ROS scavenger, and NDGA, which inhibits LOX-mediated ROS generation. Antioxidant treatments markedly reduced serum-independent cell growth (Fig. 7C) and both the number and size of the foci formed by v-Src NIH 3T3 cells after 10 days of growth in soft agar (Fig. 7D). Loss of cell viability and toxicity of NAC and NDGA were not observed in the MTT and lactate dehydrogenase assays, respectively (data not shown). Since in vitro cell proliferation does not always correlate with cell growth in vivo, solid tumor formation was analyzed by the subcutaneous injection of cells into athymic nude mice (Fig. 7E). v-Src expression causes the formation of large tumors which become evident at 8 days postinjection, whereas control NIH 3T3 cells did not form tumors. The daily treatment of mice with NDGA

described for panel C, except that immunoblotting was performed with anti-phospho-Src (Tyr527) antibodies. S, suspended cells; A, adherent cells. (E) To analyze the phosphorylation of p125FAK, cells were treated as described for panel A, except that p125FAK was immunoprecipitated. Immunoprecipitates were separated by 8% SDS-PAGE, and antiphosphotyrosine immunoblotting was performed. The blot was then stripped and reprobed with anti-p125FAK antibodies for normalization. The histogram shows the data obtained from the densitometric analysis of both blots. Susp, suspended cells; Adh 45, adherent cells. All these data are representative of at least three independent experiments.

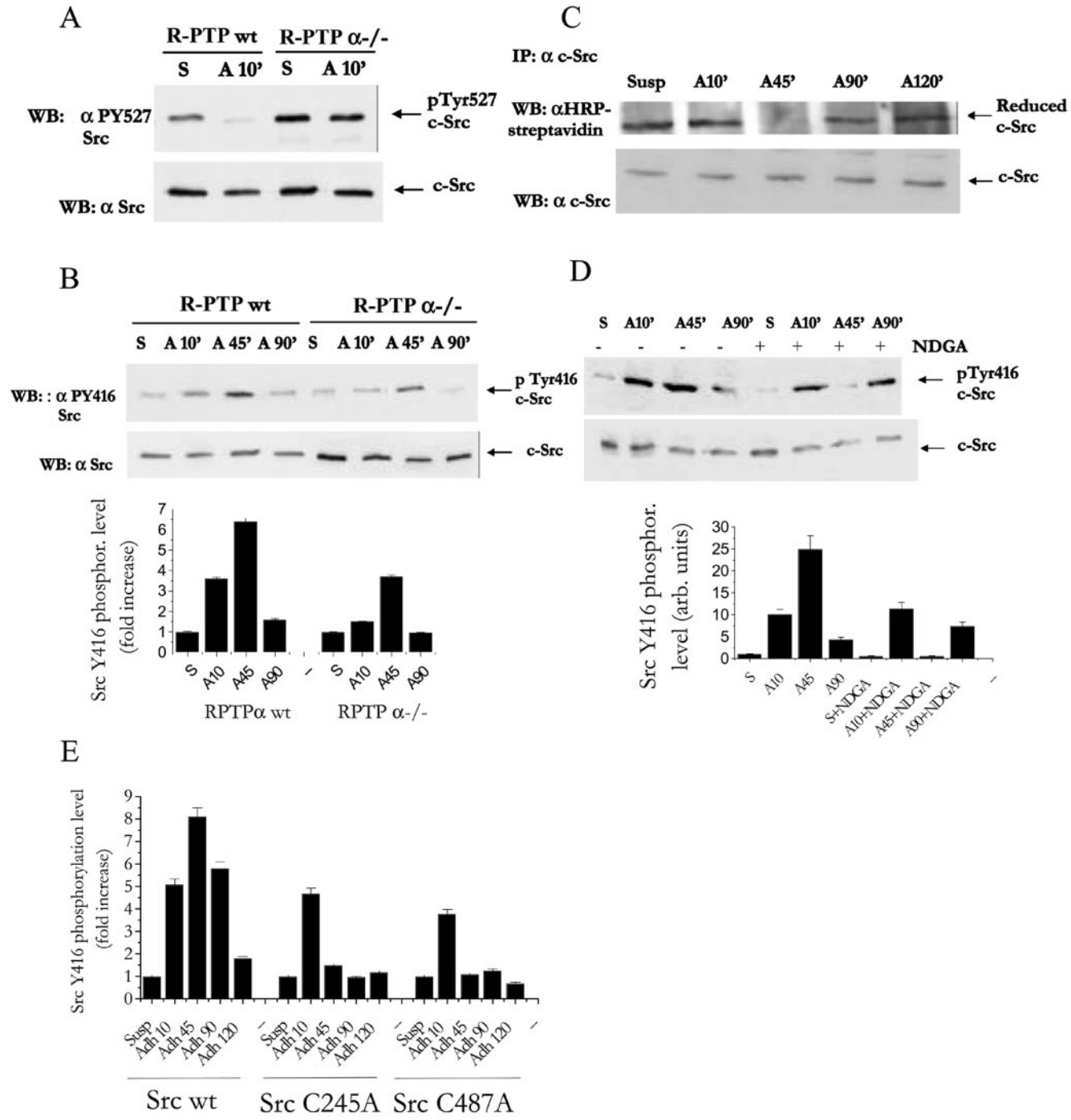

FIG. 5. Early and late Src activation due to ECM contact: differential role of Tyr527 dephosphorylation and ROS. (A) R-PTPα$^{-/-}$ cells and R-PTPα wt cells (1×10^6) were serum starved for 24 h. After detachment and 30 min of suspension at 37°C, cells were kept in suspension or seeded onto fibronectin-treated dishes for 10 min. Twenty-five micrograms of total lysate in cRIPA buffer was separated by 10% SDS-PAGE, and immunoblotting (WB) was performed with anti-phospho-Src (Tyr527) or with c-Src antibodies for normalization. (B) R-PTPα$^{-/-}$ cells and R-PTPα wt cells (1×10^6) were serum starved for 24 h. After detachment and 30 min of suspension at 37°C, cells were kept in suspension or seeded onto fibronectin-treated dishes for the indicated times. Twenty-five micrograms of total lysate in cRIPA buffer was separated by 10% SDS-PAGE, and immunoblotting was performed with anti-phospho-Src (Tyr416) or with c-Src antibodies for normalization. The bar plot shows the normalized data obtained from the densitometric analysis of both blots. (C) NIH 3T3 cells were serum starved for 24 h and then detached and maintained in suspension with gentle agitation for 30 min at 37°C. Cells were then kept in suspension or replated onto fibronectin-precoated dishes for the indicated times. c-Src was immunoprecipitated from BIAM-labeled cell lysates. HRP-streptavidin and anti-c-Src immunoblotting was performed. (D) NIH 3T3 cells (1×10^6) were treated as described for panel C, except that they were pretreated for 30 min until adhesion with or without 10 μM NDGA to inhibit the LOX-mediated synthesis of ROS. Cells were lysed in 0.5 ml of cold cRIPA lysis buffer. Twenty-five micrograms of total protein for each sample was separated by 10% SDS-PAGE, and immunoblotting was performed with anti-phospho-Src (Tyr416) or with c-Src

causes both a delay in tumor onset and a decrease in tumor volume.

To confirm the role for the oxidation of Cys245 and Cys487 in the oncoproperties of v-Src kinase, we stably overexpressed the SrcY527F oncoprotein and its C245 and C478 mutants (Y527F-C245A and Y527F-C487A, respectively) in NIH 3T3 cells (Fig. 8A). The production of ROS in Y527FSrc NIH 3T3 cells is actually very similar to that in v-Src NIH 3T3 cells (see Fig. S3 in the supplemental material). The substitution of these two cysteine residues completely abolishes the oncoproperties of SrcY527F, namely, the round shape of the cell (Fig. 8B), serum-independent growth (Fig. 8C), anchorage-independent growth (Fig. 8D), and invasivity (Fig. 8E). Taken together, these results support the conclusion that ROS-mediated oxidation of v-Src is required for its tumorigenic properties, such as invasiveness through basal laminas, anchorage- and serum-independent growth, and tumor formation in vivo.

DISCUSSION

The current study contributes to the general idea of ROS as key second messengers during cell adhesion and spreading. In this report, we propose that the tyrosine kinase Src, along with the previously described SH2 and SH3 displacement activation switches, undergoes redox regulation during cell adhesion, leading to its activation. These data lead to two major conclusions. (i) The redox-dependent Src activation is concurrent with the maximal integrin-elicited ROS burst during cell spreading and contributes to the late activation of the kinase. (ii) Src redox regulation is a key feature of the oncogenic properties of the kinase, with both the in vitro invasiveness and the transformation-dependent cell proliferation of the tyrosine kinase being dependent upon ROS production.

We therefore propose a novel in vivo redox switch that, along with the already known C-terminal tyrosine dephosphorylation and SH2/SH3 recruiting activation systems (5, 15), acts during cell adhesion to the ECM to organize the cytoskeleton. We report that Src is directly oxidized in response to ECM contact, strictly concomitantly with the ROS boost that happens 45 min after integrin receptor stimulation. This oxidation leads to the enhanced activation of c-Src, as indicated by an enzymatic assay and evaluation of the phosphorylation of Tyr416 in the activation loop. Our data indicate that c-Src oxidation involves two sulfhydryl groups, namely, Cys245 in the SH2 domain and Cys487 in the kinase domain. We propose that redox regulation is a central feature of Src function in response to ECM contact, as the elimination of ROS by antioxidant treatment almost completely abolishes Src activation. This proposal is further supported by the ability of antioxidants to inhibit p125FAK/Src association and p125FAK phosphorylation and is in agreement with previously reported data show-

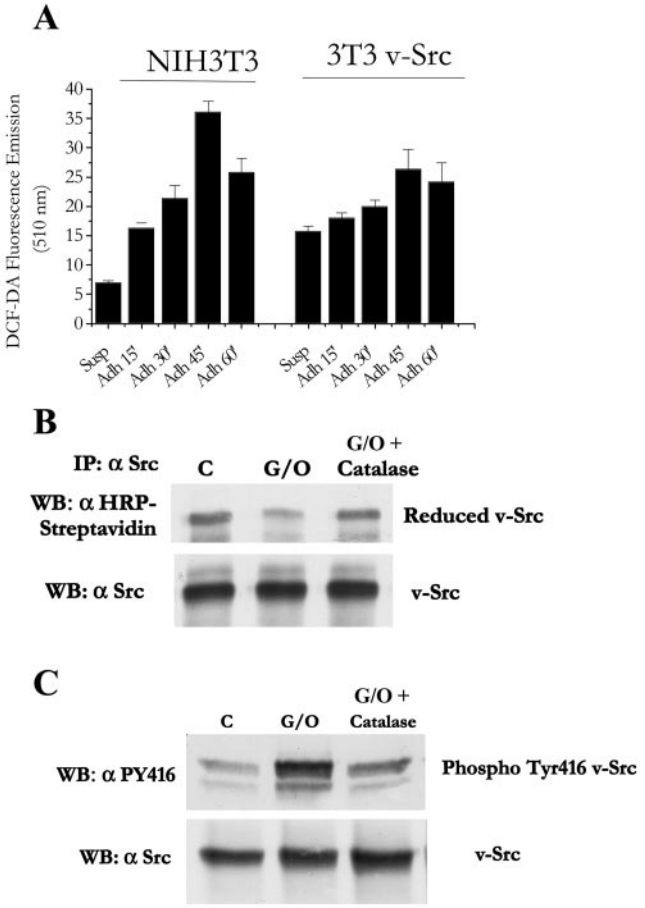

FIG. 6. v-Src oxidation and activation. (A) v-Src NIH 3T3 and NIH 3T3 cells (1×10^6) were serum starved for 24 h before being detached and maintained in suspension with gentle agitation for 30 min at 37°C. Cells were then kept in suspension (Susp) or seeded onto plastic culture dishes (Adh) for the indicated times. Hydrogen peroxide was evaluated with DCF-DA as reported in Materials and Methods. (B) v-Src NIH 3T3 cells (1×10^6) were serum starved for 24 h and then stimulated with or without 100 mU/ml G/O for 15 min. In one sample, the medium was changed and 1 μg/ml of PEG catalase was added for 30 min. Cell lysates were labeled with 40 μM BIAM, and v-Src was immunoprecipitated from each sample. The samples were split in two, and HRP-streptavidin and anti-Src immunoblotting (WB) was performed. (C) To analyze Src activation, cells were treated as described for panel A, except that cells were lysed in 0.5 ml of cold cRIPA lysis buffer. Twenty-five micrograms of total proteins for each sample was separated by 10% SDS-PAGE, and immunoblotting was performed with anti-phospho-Src (Tyr416) and with anti-Src antibodies (for normalization). All the reported experiments are representative of three others with similar results.

antibodies for normalization. The bar plot shows the normalized data obtained from the densitometric analysis of both blots. All the reported experiments are representative of three others with similar results. (E) NIH 3T3 cells (1×10^6) were transfected with pSG5 encoding wt c-Src, C245A, or C487A. Twenty-four hours after transfection, cells were serum starved for an additional 24 h before being detached and maintained in suspension for 30 min at 37°C with gentle agitation. Cells were either kept in suspension or seeded onto fibronectin-treated dishes for the indicated times. Twenty-five micrograms of total lysate in cRIPA buffer was separated by 10% SDS-PAGE, and immunoblotting was performed with anti-phospho-Src (Tyr416) or with c-Src antibodies for normalization. The histogram in panel E shows the normalized data obtained from the densitometric analysis of both the blots. S, suspended cells; A, adherent cells (for panels A through D). Susp, suspended cells; Adh, adherent cells (for panel E).

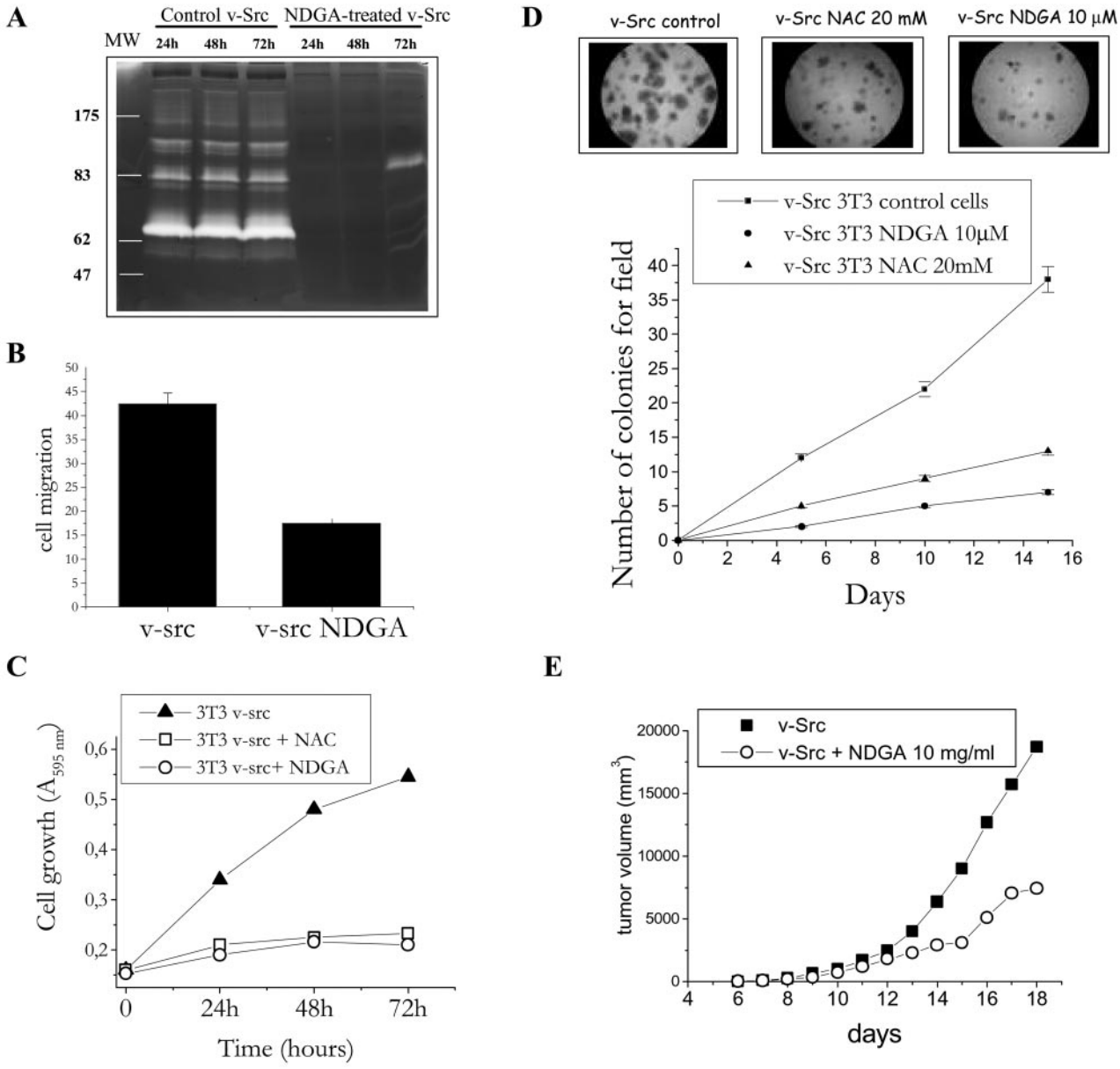

FIG. 7. Effect of v-Src redox regulation on its oncogenic properties. (A) Cells (3×10^5) of the indicated types were allowed to grow for 72 h in culture medium alone or supplemented every 24 h with 10 μM NDGA to inhibit the LOX-mediated ROS production. The medium was collected at 24 h, 48 h, and 72 h and analyzed for MMP activity by gelatin zymography. Band intensities are proportional to the levels of MMP activity on gelatin as substrate. (B) v-Src NIH 3T3 cells (1×10^5) treated with or without 10 μM NDGA were seeded into the upper chamber of a 2.5-cm transwell precoated with a Matrigel layer. Cell were allowed to migrate for 24 h toward the lower chamber filled with growth medium supplemented with 20% FCS. Cell migration was evaluated after Diff-Quick staining and reported in the histogram as the average number of cells counted in six randomly chosen fields. (C) Cells (2×10^4) of the indicated types were seeded into gelatin-coated 24-multiwell plates in 0.5% serum with or without 10 μM NDGA or 20 mM NAC. Cell growth was evaluated every 24 h by crystal violet staining. Values are means ± SD from three independent experiments. (D) Anchorage-independent cell growth in 0.3% soft agar on a solidified base was evaluated by plating 4×10^4 v-Src NIH 3T3 cells in 10% serum with or without 20 mM NAC or 10 μM NDGA. Colony formation was scored after 2 weeks of culture. Magnification, ×20. All data are representative of at least three independent experiments. (E) Tumorigenicity assays were performed by subcutaneous injection with 1×10^6 NIH 3T3 v-Src cells (six mice per treatment). Subcutaneous tumors were grossly visible at the site of injection after 6 to 8 days. Animals were examined daily and sacrificed 20 days later. The volume of the tumor in each analyzed group is reported and the mean ± SD is shown.

ing that ROS are necessary for integrin signaling during fibroblast adhesion and spreading (10, 34).

The kinetics of Src activation in response to ECM contact depicts an increase at 10 min after integrin engagement, which we termed Src early activation, followed by a slight decrease thereafter. At the time of maximal ROS production, we detect a stronger Src activation, which we refer to as the late Src response. These two phases temporally correlate with the formation of focal adhesion and podosomes and with cell spreading and reorganization of the cytoskeleton, respectively. The

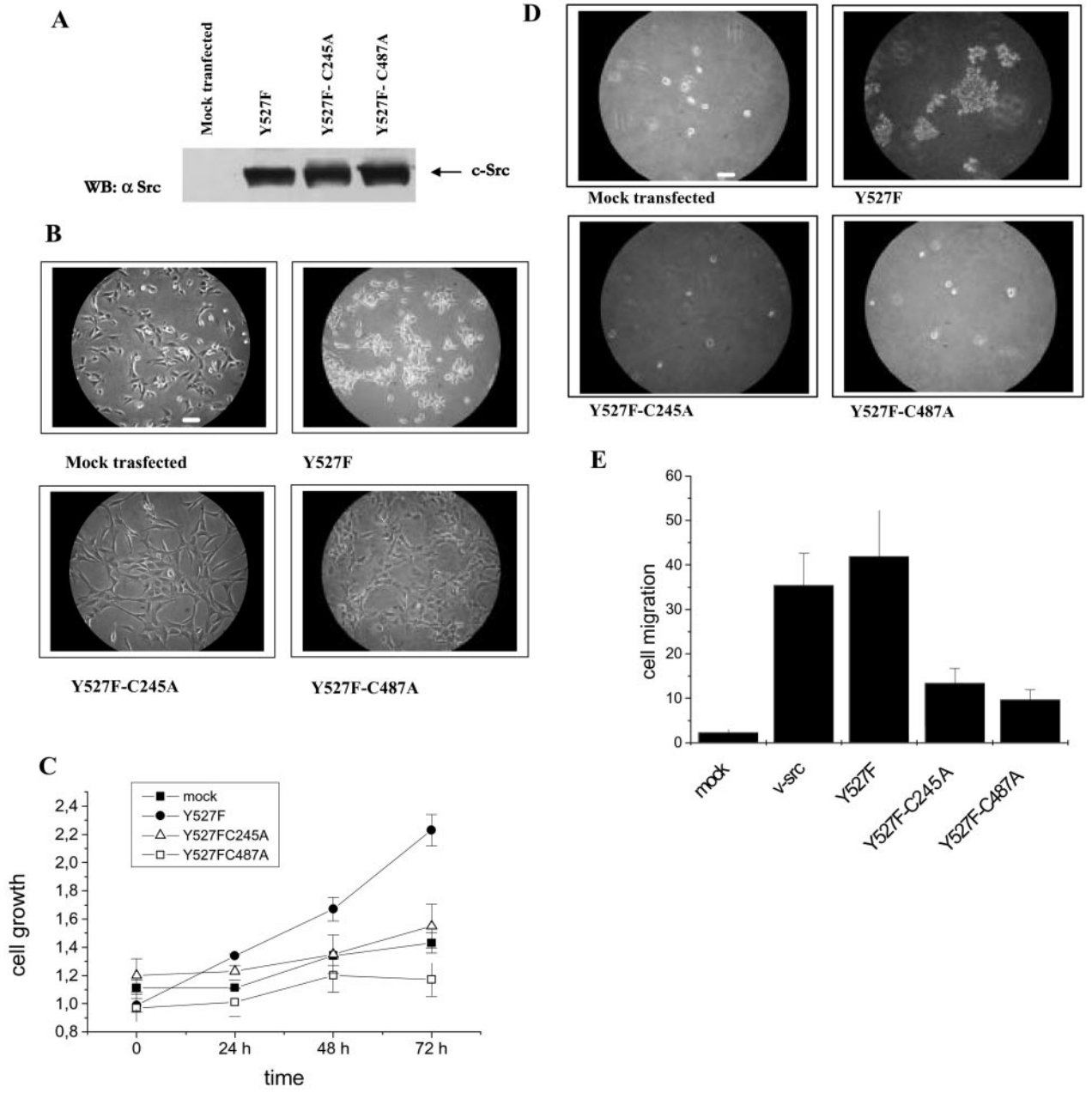

FIG. 8. Effect of C245A and C487A mutations on Src oncogenic properties. (A) The expression levels of the indicated cell types were checked by anti-Src immunoblotting (WB). (B) Cell morphology. Cells (3×10^5) of the indicated types were allowed to grow for 24 h, and then photographs of paraformaldehyde-fixed cells were taken with a phase-contrast microscope. Bar, 100 μm. (C) Serum-independent growth. Cells (2×10^4) of the indicated types were seeded into gelatin-coated 24-multiwell plates in 0.5% serum. Cell growth was evaluated every 24 h by crystal violet staining. Values are means ± SD from three independent experiments. (D) Anchorage-independent cell growth in 0.3% soft agar on a solidified base was evaluated by plating cells in 10% serum. Colony formation was scored after 2 weeks of culturing. Magnification, ×20. All data are representative of at least three independent experiments. (E) Invasion assay. Cells (1×10^5) of the indicated types were seeded into the upper chamber of a 2.5-cm transwell and precoated with a Matrigel layer. Cells were allowed to migrate for 24 h towards the lower chamber filled with growth medium supplemented with 20% FCS. Cell migration was evaluated after Diff-Quick staining and reported in the histogram as the average number of cells counted in six randomly chosen fields.

early increase in Src activity is due mainly to the dephosphorylation of C-terminal Tyr527 by membrane-associated PTPs. Although many PTPs, such as PTP1B and SH2 domain PTP2, have been indicated for this dephosphorylation (4, 38), in the context of integrin-mediated cell adhesion, the role of R-PTPα is strongly designated (29). Our data concerning the role of R-PTPα in Src activation during cell adhesion reveal that early and late activations of the kinase are two distinct phenomena. In particular, we show that cells that are impaired for early Src activation, i.e., R-PTPα$^{-/-}$ cells, are nevertheless able to acti-

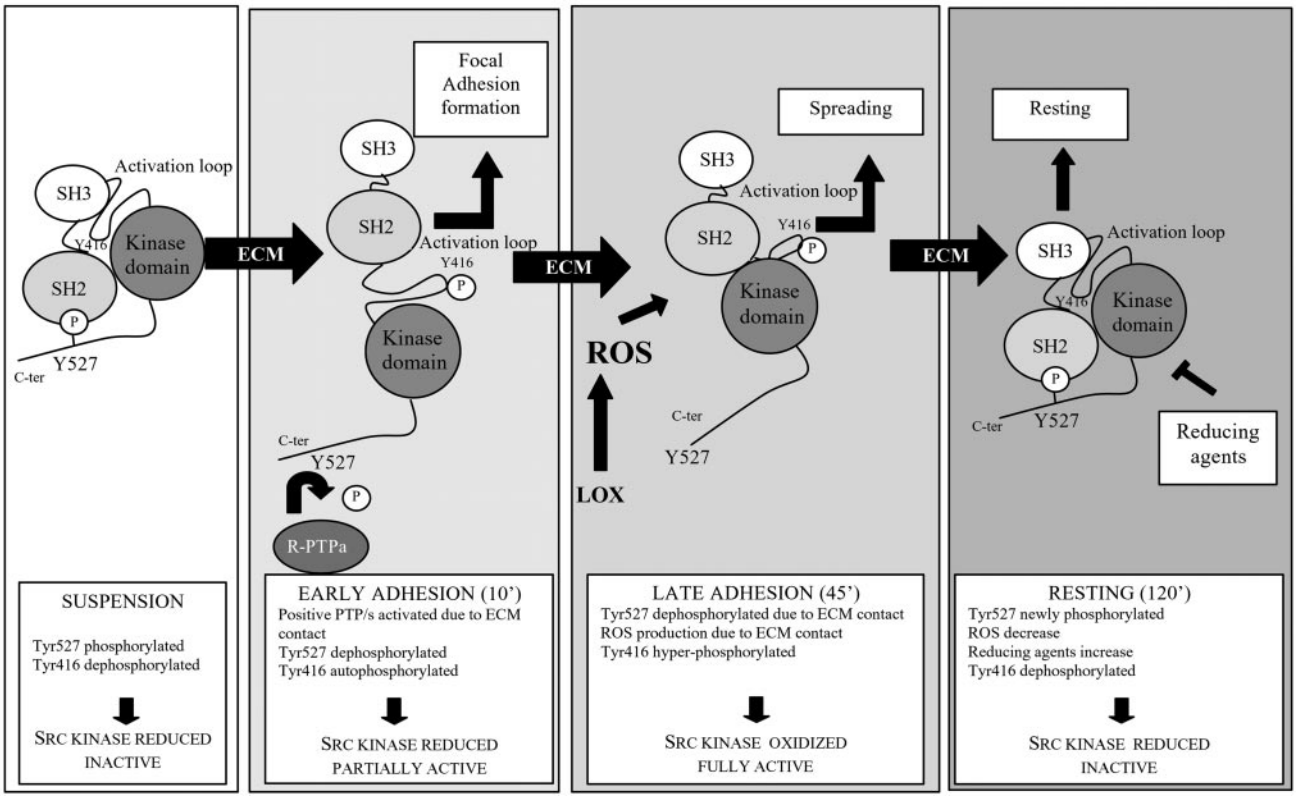

FIG. 9. Proposed model of Src activation due to ECM contact. In suspended cells, Src is in a closed inactive conformation, with the inhibitory Tyr527 phosphorylated and engaged with the SH2 domain. This closed structure maintains the activation loop Tyr416 as unavailable for autophosphorylation. At the early phase of integrin engagement by the ECM, activation by R-PTPα occurs, leading to the dephosphorylation of Tyr527 and to the conversion of the kinase to an open conformation. Tyr416 is now accessible for autophosphorylation. Kinase activity increases with the subsequent phosphorylation of several focal adhesion proteins and progress of focal adhesion formation. At this stage of adhesion, ROS concentration is not high enough to induce redox control of the Src kinase. At a later phase of cell adhesion, there is a strong increase in ROS production that leads to direct Src oxidation, which strongly increases kinase activity. This phase of Src redox regulation corresponds to cell spreading. In resting conditions, Tyr527 is newly phosphorylated, inducing Src to return to a closed conformation. In addition, ROS decrease to a basal level, thus inducing Src rereduction. Times of adhesion (in min) are indicated. C-ter, C terminus.

vate Src later on, in strict concomitance with the rise in ROS levels. In keeping with the role of Src oxidation in the late phase of integrin-mediated cell adhesion, we reported that Cys245 and Cys487 Src mutants are dually resistant to oxidation and late activation, yet still undergo early activation and Tyr527 dephosphorylation, suggesting that these two cysteines do not play any role in the early phase of cell adhesion. In this sense, Cys245A and Cys487A Src mutants behave as ROS-insensitive Src molecules.

An intriguing possibility that follows from our present data is that the dephosphorylation-mediated early activation, although a separate step, may facilitate the late ROS-mediated Src activation. In fact, the extents of late Src activation differ slightly between R-PTPα-deficient cells and wild-type cells, suggesting that the switch to an open conformation achieved upon Tyr527 dephosphorylation is a relevant step in the fostering of the subsequent direct oxidation of the Src kinase

Integration of these findings with published reports on Src activation allows us to propose a new comprehensive model of Src activation during ECM contact (Fig. 9). In suspended cells, Src is in its inactive form, phosphorylated at C-terminal Tyr527. This closed structure positions the activation loop Tyr416 so that it is unavailable for the kinase domain. The first contact with the ECM induces the dephosphorylation of Tyr527 by R-PTPα and the opening of the closed Src structure. The SH2 domain is now free to recruit phosphorylated proteins, driving the assembly of focal adhesions. The activation loop contacts the kinase domain, and Tyr416 is autophosphorylated. This is a redox-independent Src activation step, which we labeled early activation. Thereafter, continued integrin engagement gives rise to an ROS increase and oxidation of Src kinase and thus to Src activation through an increase of Tyr416 phosphorylation. This redox-dependent step in Src activation overlaps with cell spreading. Upon a return to resting conditions, the redox potential newly decreases, Src is rereduced, and Tyr527 is rephosphorylated, leading Src to its closed inactive form.

The functional role of Src redox regulation is underlined by our findings on in vitro and in vivo tumorigenic properties of v-Src tyrosine kinase. We demonstrated that the production of ROS is crucial for MMP expression, chemoinvasivity, three-dimensional cell motility, and serum- and anchorage-independent growth induced by v-Src transformation. In keeping with our hypothesis, the mutation of Cys245 or Cys487 dramatically

reduces chemoinvasivity and GF- and anchorage-dependent growth induced by oncogenic Y527FSrc. The lack of the C-terminal Tyr527 in the v-Src oncoprotein leads to basal kinase activation and has been indicated as the key effector of the pleiotropic oncogenic effects of v-Src (18). In addition, in metastases of human colon cancer, c-Src acquires transforming ability due to mutations at the Tyr527 site (20, 25). Our results shed now new light on the synergistic action of Src redox regulation and C-terminal Tyr527 dephosphorylation as global switches for Src-mediated cell transformation. We would like to underline that, although integrin-dependent ROS are mandatory for the full activation of c-Src kinase, needing both step 1 (dephosphorylation) and step 2 (oxidation), in v-Src the kinase is basally activated for two reasons, namely, the lack of P-Tyr527 inhibition and the high level of ROS observed in v-Src transformed cells, and thereby induces the kinase oxidation. In both cases, ROS cooperate to yield a fully active kinase. We propose that excess ROS production associated with cell transformation (6, 30) could initiate costimulatory signals that are normally triggered by cell/ECM interaction and may correlate with v-Src tumorigenic potential. Considering that the anchorage-independent growth of Src-transformed cells directly correlates with their metastatic potentials (21, 25), this report opens new avenues for antioxidant-based pharmacological intervention in anchorage-independent Src-mediated cell transformation.

ACKNOWLEDGMENTS

This work was supported by the Italian Association for Cancer Research (AIRC), by the Ministero della Università e Ricerca Scientifica e Tecnologica (MIUR-PRIN 2002), by Consorzio Interuniversitario Biotecnologie, and by Cassa di Risparmio di Firenze.

We thank Alan Levine for helpful discussion and critical reading of the manuscript.

REFERENCES

1. **Aslan, M., and T. Ozben.** 2003. Oxidants in receptor tyrosine kinase signal transduction pathways. Antioxid. Redox Signal. **5:**781–788.
2. **Atfi, A., E. Drobetsky, M. Boissonneault, A. Chapdelaine, and S. Chevalier.** 1994. Transforming growth factor beta down-regulates Src family protein tyrosine kinase signaling pathways. J. Biol. Chem. **269:**30688–30693.
3. **Benhar, M., D. Engelberg, and A. Levitzki.** 2002. ROS, stress-activated kinases and stress signaling in cancer. EMBO Rep. **3:**420–425.
4. **Bjorge, J. D., A. Pang, and D. J. Fujita.** 2000. Identification of protein-tyrosine phosphatase 1B as the major tyrosine phosphatase activity capable of dephosphorylating and activating c-Src in several human breast cancer cell lines. J. Biol. Chem. **275:**41439–41446.
5. **Brown, M. T., and J. A. Cooper.** 1996. Regulation, substrates and functions of src. Biochim. Biophys. Acta **1287:**121–149.
6. **Burdon, R. H.** 1995. Superoxide and hydrogen peroxide in relation to mammalian cell proliferation. Free Radic. Biol. Med. **18:**775–794.
7. **Chiarugi, P., and P. Cirri.** 2003. Redox regulation of protein tyrosine phosphatases during receptor tyrosine kinase signal transduction. Trends Biochem. Sci. **28:**509–514.
8. **Chiarugi, P., P. Cirri, M. L. Taddei, D. Talini, L. Doria, T. Fiaschi, F. Buricchi, E. Giannoni, G. Camici, G. Raugei, and G. Ramponi.** 2002. New perspectives in PDGF receptor downregulation: the main role of phosphotyrosine phosphatases. J. Cell Sci. **115:**2219–2232.
9. **Chiarugi, P., T. Fiaschi, M. L. Taddei, D. Talini, E. Giannoni, G. Raugei, and G. Ramponi.** 2001. Two vicinal cysteines confer a peculiar redox regulation to low molecular weight protein tyrosine phosphatase in response to platelet-derived growth factor receptor stimulation. J. Biol. Chem. **276:**33478–33487.
10. **Chiarugi, P., G. Pani, E. Giannoni, L. Taddei, R. Colavitti, G. Raugei, M. Symons, S. Borrello, T. Galeotti, and G. Ramponi.** 2003. Reactive oxygen species as essential mediators of cell adhesion: the oxidative inhibition of a FAK tyrosine phosphatase is required for cell adhesion. J. Cell Biol. **161:**933–944.
11. **Cooper, J. A., and B. Howell.** 1993. The when and how of Src regulation. Cell **73:**1051–1054.
12. **Cunnick, J. M., J. F. Dorsey, T. Standley, J. Turkson, A. J. Kraker, D. W. Fry, R. Jove, and J. Wu.** 1998. Role of tyrosine kinase activity of epidermal growth factor receptor in the lysophosphatidic acid-stimulated mitogen-activated protein kinase pathway. J. Biol. Chem. **273:**14468–14475.
13. **Finkel, T.** 2001. Reactive oxygen species and signal transduction. IUBMB Life **52:**3–6.
14. **Frame, M. C., V. J. Fincham, N. O. Carragher, and J. A. Wyke.** 2002. v-Src's hold over actin and cell adhesions. Nat. Rev. Mol. Cell Biol. **3:**233–245.
15. **Gonfloni, S., J. C. Williams, K. Hattula, A. Weijland, R. K. Wierenga, and G. Superti-Furga.** 1997. The role of the linker between the SH2 domain and catalytic domain in the regulation and function of Src. EMBO J. **16:**7261–7271.
16. **Haklar, G., E. Sayin-Ozveri, M. Yuksel, A. O. Aktan, and A. S. Yalcin.** 2001. Different kinds of reactive oxygen and nitrogen species were detected in colon and breast tumors. Cancer Lett. **165:**219–224.
17. **Hamaguchi, M., S. Yamagata, A. A. Thant, H. Xiao, H. Iwata, T. Mazaki, and H. Hanafusa.** 1995. Augmentation of metalloproteinase (gelatinase) activity secreted from Rous sarcoma virus-infected cells correlates with transforming activity of src. Oncogene **10:**1037–1043.
18. **Hunter, T., and J. A. Cooper.** 1985. Protein-tyrosine kinases. Annu. Rev. Biochem. **54:**897–930.
19. **Hurley, T. R., R. Hyman, and B. M. Sefton.** 1993. Differential effects of expression of the CD45 tyrosine protein phosphatase on the tyrosine phosphorylation of the lck, fyn, and c-src tyrosine protein kinases. Mol. Cell. Biol. **13:**1651–1656.
20. **Irby, R. B., W. Mao, D. Coppola, J. Kang, J. M. Loubeau, W. Trudeau, R. Karl, D. J. Fujita, R. Jove, and T. J. Yeatman.** 1999. Activating SRC mutation in a subset of advanced human colon cancers. Nat. Genet. **21:**187–190.
21. **Johnson, D., M. C. Frame, and J. A. Wyke.** 1998. Expression of the v-Src oncoprotein in fibroblasts disrupts normal regulation of the CDK inhibitor p27 and inhibits quiescence. Oncogene **16:**2017–2028.
22. **Kato, M., T. Iwashita, K. Takeda, A. A. Akhand, W. Liu, M. Yoshihara, N. Asai, H. Suzuki, M. Takahashi, and I. Nakashima.** 2000. Ultraviolet light induces redox reaction-mediated dimerization and superactivation of oncogenic Ret tyrosine kinases. Mol. Biol. Cell **11:**93–101.
23. **Mott, J. D., C. L. Thomas, M. T. Rosenbach, K. Takahara, D. S. Greenspan, and M. J. Banda.** 2000. Post-translational proteolytic processing of procollagen C-terminal proteinase enhancer releases a metalloproteinase inhibitor. J. Biol. Chem. **275:**1384–1390.
24. **Nimnual, A. S., L. J. Taylor, and D. Bar-Sagi.** 2003. Redox-dependent downregulation of Rho by Rac. Nat. Cell Biol. **5:**236–241.
25. **Russello, S. V., and S. K. Shore.** 2003. Src in human carcinogenesis. Front. Biosci. **8:**S1068–S1073.
26. **Sabe, H., M. Hamaguchi, and H. Hanafusa.** 1997. Cell to substratum adhesion is involved in v-Src-induced cellular protein tyrosine phosphorylation: implication for the adhesion-regulated protein tyrosine phosphatase activity. Oncogene **14:**1779–1788.
27. **Schwartz, M. A., and M. H. Ginsberg.** 2002. Networks and crosstalk: integrin signalling spreads. Nat. Cell Biol. **4:**E65–E68.
28. **Simon, A. R., U. Rai, B. L. Fanburg, and B. H. Cochran.** 1998. Activation of the JAK-STAT pathway by reactive oxygen species. Am. J. Physiol. **275:**C1640–C1652.
29. **Su, J., M. Muranjan, and J. Sap.** 1999. Receptor protein tyrosine phosphatase alpha activates Src-family kinases and controls integrin-mediated responses in fibroblasts. Curr. Biol. **9:**505–511.
30. **Szatrowski, T. P., and C. F. Nathan.** 1991. Production of large amounts of hydrogen peroxide by human tumor cells. Cancer Res. **51:**794–798.
31. **Tatosyan, A. G., and O. A. Mizenina.** 2000. Kinases of the Src family: structure and functions. Biochemistry (Moscow) **65:**49–58.
32. **Ushio-Fukai, M., R. W. Alexander, M. Akers, Q. Yin, Y. Fujio, K. Walsh, and K. K. Griendling.** 1999. Reactive oxygen species mediate the activation of Akt/protein kinase B by angiotensin II in vascular smooth muscle cells. J. Biol. Chem. **274:**22699–22704.
33. **von Wichert, G., G. Jiang, A. Kostic, K. De Vos, J. Sap, and M. P. Sheetz.** 2003. RPTP-α acts as a transducer of mechanical force on α_v/β_3-integrin-cytoskeleton linkages. J. Cell Biol. **161:**143–153.
34. **Werner, E., and Z. Werb.** 2002. Integrins engage mitochondrial function for signal transduction by a mechanism dependent on Rho GTPases. J. Cell Biol. **158:**357–368.
35. **Xu, D., I. I. Rovira, and T. Finkel.** 2002. Oxidants painting the cysteine chapel: redox regulation of PTPs. Dev. Cell **2:**251–252.
36. **Xu, W., S. C. Harrison, and M. J. Eck.** 1997. Three-dimensional structure of the tyrosine kinase c-Src. Nature **385:**595–602.
37. **Yagel, S., A. H. Warner, H. N. Nellans, P. K. Lala, C. Waghorne, and D. T. Denhardt.** 1989. Suppression by cathepsin L inhibitors of the invasion of amnion membranes by murine cancer cells. Cancer Res. **49:**3553–3557.
38. **Zhang, S. Q., W. Yang, M. I. Kontaridis, T. G. Bivona, G. Wen, T. Araki, J. Luo, J. A. Thompson, B. L. Schraven, M. R. Philips, and B. G. Neel.** 2004. Shp2 regulates SRC family kinase activity and Ras/Erk activation by controlling Csk recruitment. Mol. Cell **13:**341–355.
39. **Zheng, X. M., R. J. Resnick, and D. Shalloway.** 2000. A phosphotyrosine displacement mechanism for activation of Src by PTPalpha. EMBO J. **19:**964–978.